Pre-launch estimates for GLAST sensitivity to Dark Matter annihilation signals

E.A. Baltz, B. Berenji, G. Bertone, L. Bergström , E. Bloom, T. Bringmann , J. Chiang, J. Cohen-Tanugi, J. Conrad , Y. Edmonds, J. Edsjö, G. Godfrey, R. E. Hughes, R. P. Johnson, A. Lionetto, A. A. Moiseev, A. Morselli, I. V. Moskalenko, E. Nuss, J. F. Ormes, R. Rando, A. J. Sander, A. Sellerholm, P. D. Smith, A. W. Strong, L. Wai, P. Wang, B. L. Winer, arXiv:0806.2911

Masaki Mori

ICRR CANGAROO group internal seminar, July 24, 2008

GLAST LAT Instrument

- Tracker: conversion, tracking.
  - Angular resolution is dominated by scattering.
  - Converter thickness optimization.
- Calorimeter: energy measurement.
  - 8.4 radiation length.
  - Use shower development to compensate for the leak.
- Anti-coincidence detector:
  - Efficiency > 99.97%.
- Total mass < 3000 kg.
- Active Area > 1.9 m^2.
- Total power < 650 W.
- Orbit: 575 km altitude.
  - ~25° inclination.

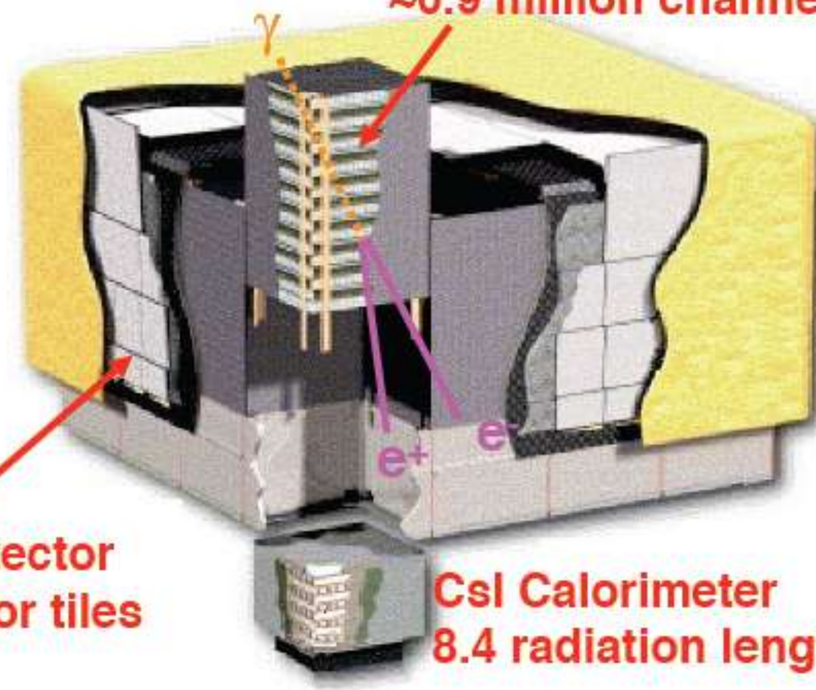

Studies of Cosmic-Rays with GeV Gamma-Rays,
H. Tajima, Cosmic-rays and High Energy Universe, Mar 6, 2007

Successfully launched on June 11, 2008

GLAST LAT Performance Summary

- Energy range: 20 MeV – 300 GeV (*e*: >30 GeV)
- Energy Resolution: ~10% (~5% off-axis)
- PSF (68%) at 100 MeV ~ 5° (W thickness)
- PSF (68%) at 10 GeV ~ 0.1° (SSD resolution)
- Field Of View: 2.4 sr (All sky monitor)
- Point Source sens. (>100 MeV): 3×10^{-9} cm $^{-2}$ s^{-1} (>30 times better than EGRET)
- Dead time: < 30 μs (GRB science)

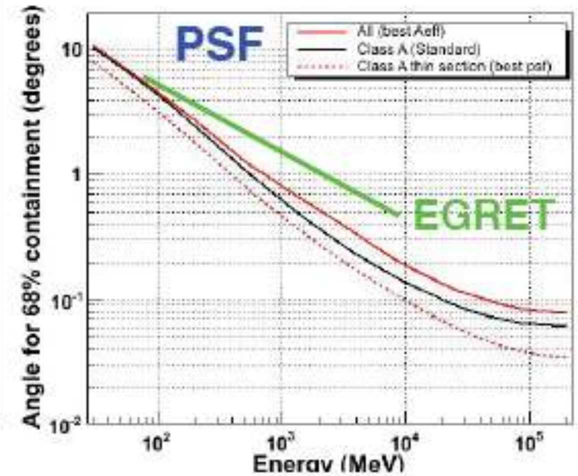

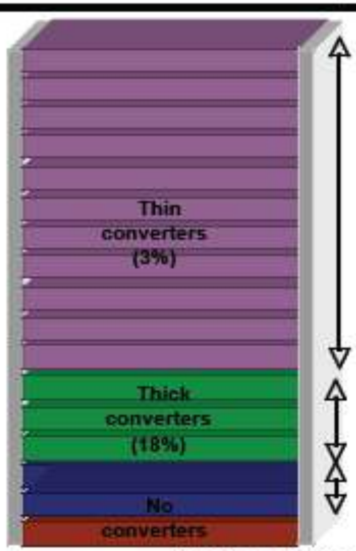

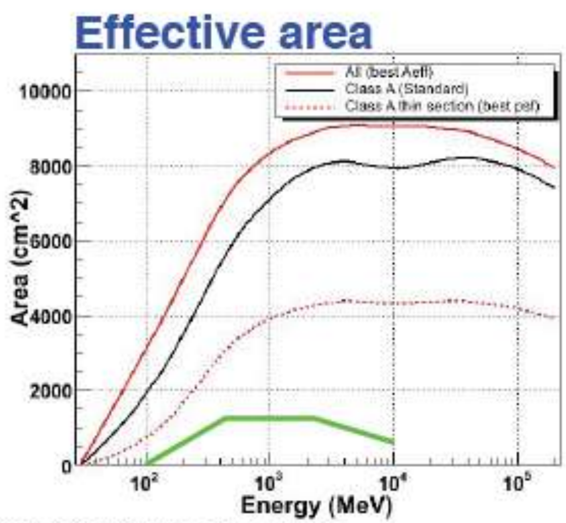

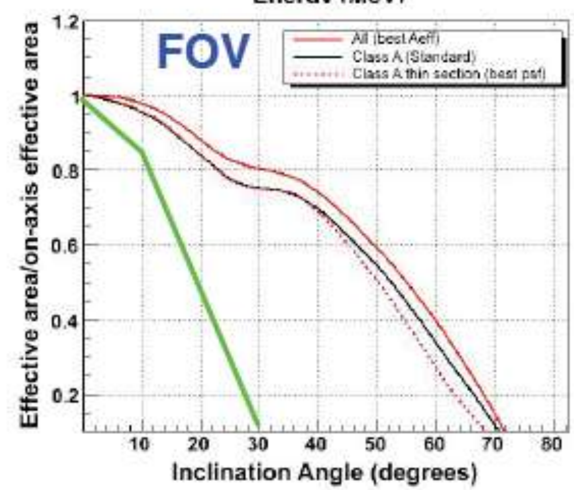

Studies of Cosmic-Rays with GeV Gamma-Rays,
H. Tajima,Cosmic-rays and High Energy Universe, Mar 6, 2007

Sample event display

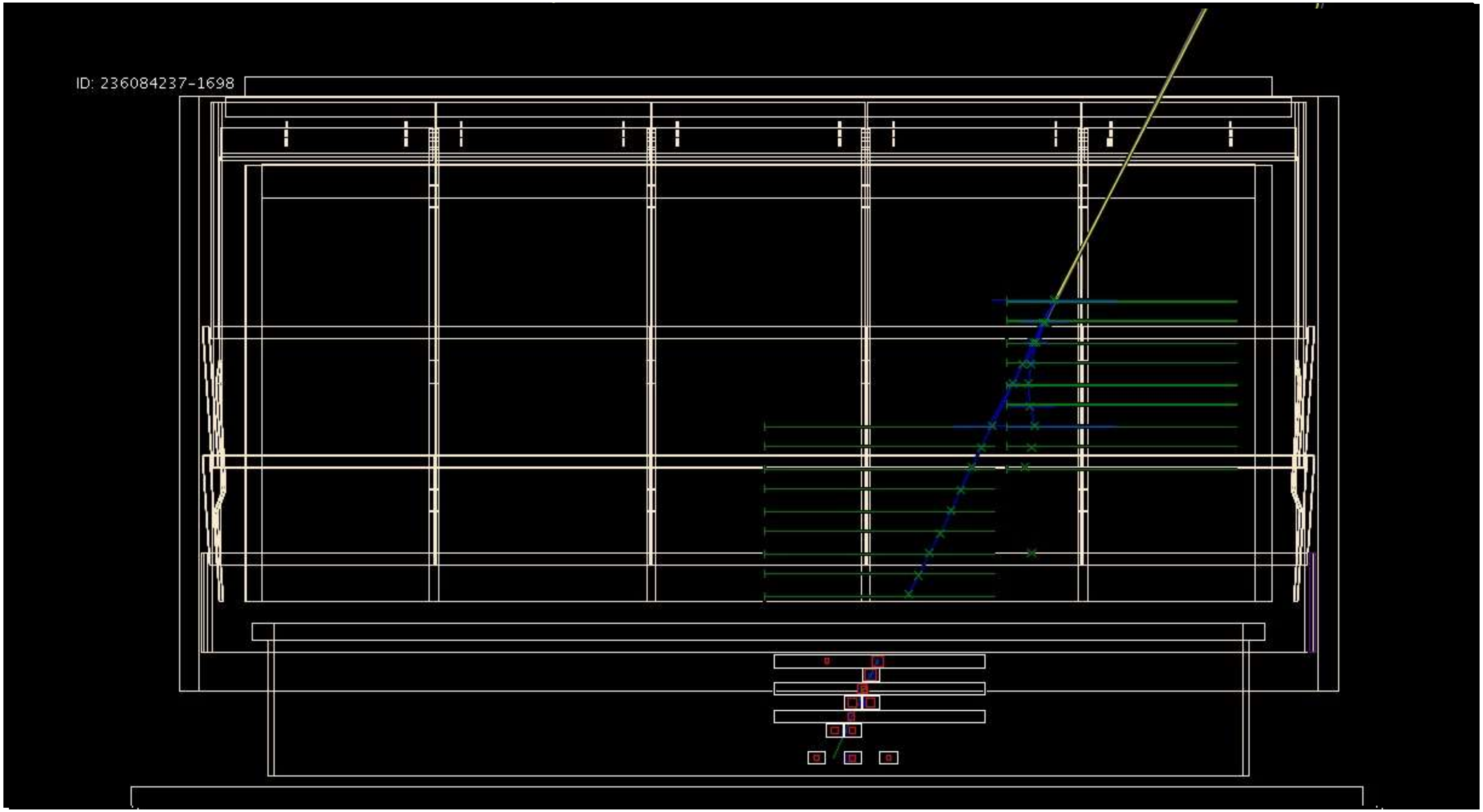

http://www-glast.stanford.edu/WiredAnimation/

Particle dark matter or WIMPs

- Cold Dark Matter
  - Combined study of the cosmic microwave background radiation, supernova cosmology and large Galaxy redshift surveys that non-baryonic dark matter is needed.
- WIMP (Weakly Interacting Massive Particle)
  - Lightest supersymmetric partner (LSP)
  - Kaluza-Klein models
  - Universal Extra Dimension models
- "WIMP miracle"
  - Not much fine tuning necessary to account for $\Omega_{CDM} h^2 \sim 0.1$

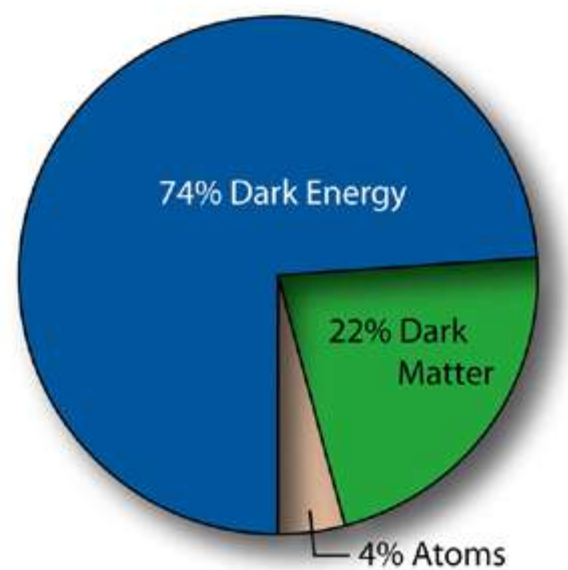

Gamma-ray production from WIMPs

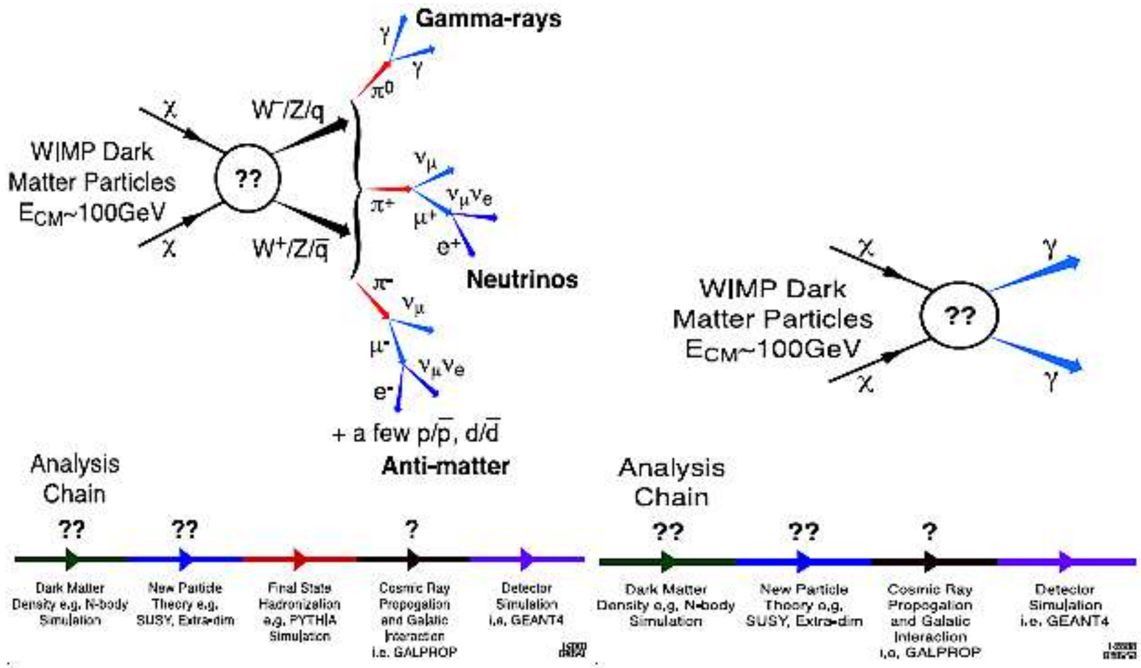

Figure 1. A diagrammatic flow of how gamma rays are produced by annihilation of dark matter and elements of the analysis chain used by the GLAST collaboration to detect them. The double question mark in the simulation chain indicates high uncertainty in the models of dark matter density and the new particle theories discussed in the paper. The single question mark over the cosmic ray propagation and interaction models indicates lesser, although significant, uncertainty in those models that generate backgrounds to the potential dark matter gamma ray signal. In this paper GALPROP (section 3.2) is used to estimate those backgrounds. In the next step, γ-ray detection is simulated using standard detector simulation packages (GEANT 4). Finally,these simulated LAT events are treated by various analysis software programs (event reconstruction and statistical analysis) to generate the results presented in this work. The same procedure is applied to the smoking gun signal of $\chi\chi \to \gamma\gamma$, except that in this case hadronization does not have to be taken into account.

Various method

Table 1. *The various venues GLAST will explore in its search for WIMPs, and the advantage/disadvantage of each method.*

Search	Advantages	Challenges
Galactic center	Good statistics	Source confusions Uncertainty in diffuse background prediction
Satellites	Low background, good source identification	Astrophysical Uncertainties
Galactic halo	Very good statistics	Uncertainties in Galactic diffuse background prediction
Extra galactic	very good statistics	Uncertainties in Galactic diffuse contribution Astrophysical uncertainties
Spectral lines	No astrophysical uncertainties "Smoking gun" signal	Potentially low statistics

GLAST exposure in 5 years

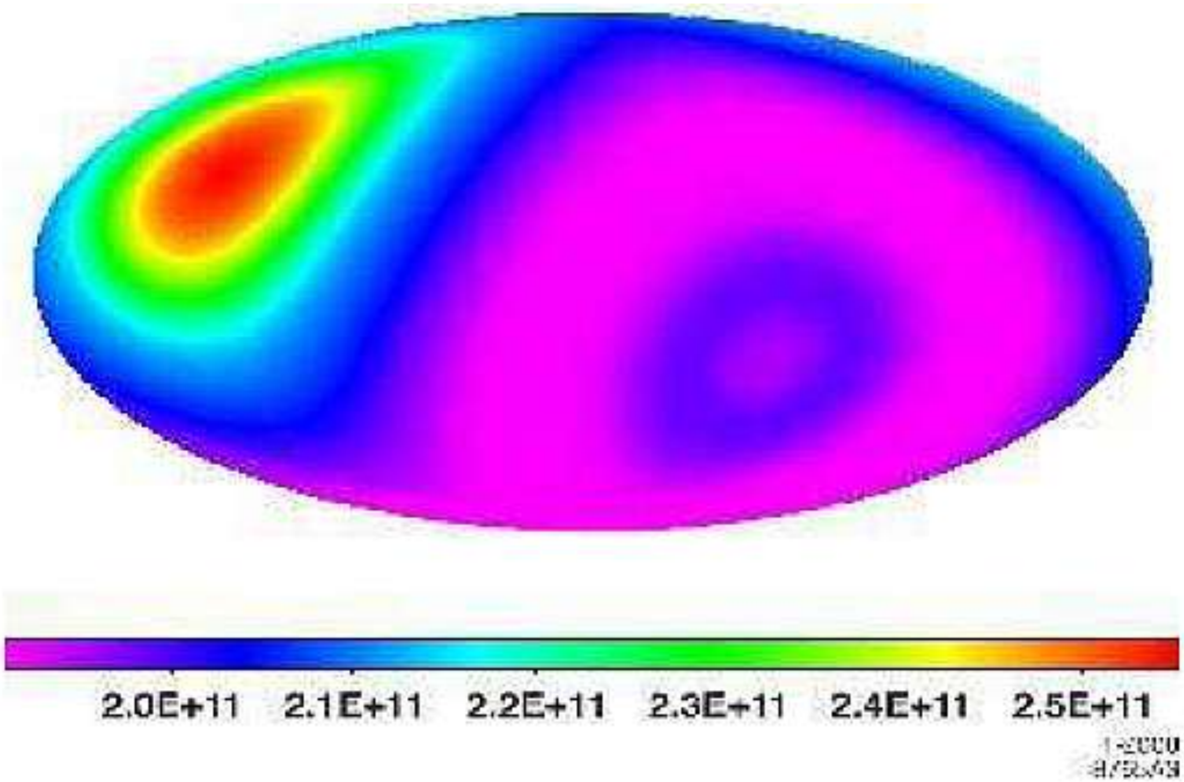

Almost uniform within ±15%

Figure 2. The simulated LAT exposure, in units of cm^2 sec, **for 5 years of all-sky scan.** The effect of turning off the LAT while in the SAA is included in the exposure. This exposure is calculated for a photon energy of 100 GeV. The plot is in Galactic coordinates with the values of exposure shown on the grey (coloured in coloured versions of the paper) bar in units of cm^2 sec.

Gamma-ray signal

- Gamma-ray flux from G.C.

$$\phi_{WIMP}(E,\psi) = \frac{1}{2}\frac{<\sigma v>}{4\pi}\sum_f \frac{dN_f}{dE}B_f \int_{\mathrm{l.o.s}} dl(\psi)\frac{\rho(l)^2}{m_{WIMP}^2} \ .$$

  σ: annihilation cross section, v: relative velocity, dN_f/dE: photon yields, B_f: branching ration, ψ:angle from G.C., ρ: density, integral over line-of-sight

- Dominant modes in annihilation: $b\bar{b}, t\bar{t}, \tau^+\tau^-, W^+W^-, Z^0Z^0$ (s-wave annihilation $\propto m_f^2/m_{\mathrm{WIMP}}^2$)
- Density distribution in halos $\rho(r) = \dfrac{\rho_s}{\left(\frac{r}{r_s}\right)^\gamma \left(1+\left(\frac{r}{r_s}\right)^\alpha\right)^{(\beta-\gamma)/\alpha}}$

  $(\alpha,\beta,\gamma,r_s)$=(1,3,1,20kpc)[NFW], (1,3,1.5,28kpc) [Moore]

Density profile: Moore vs NFW

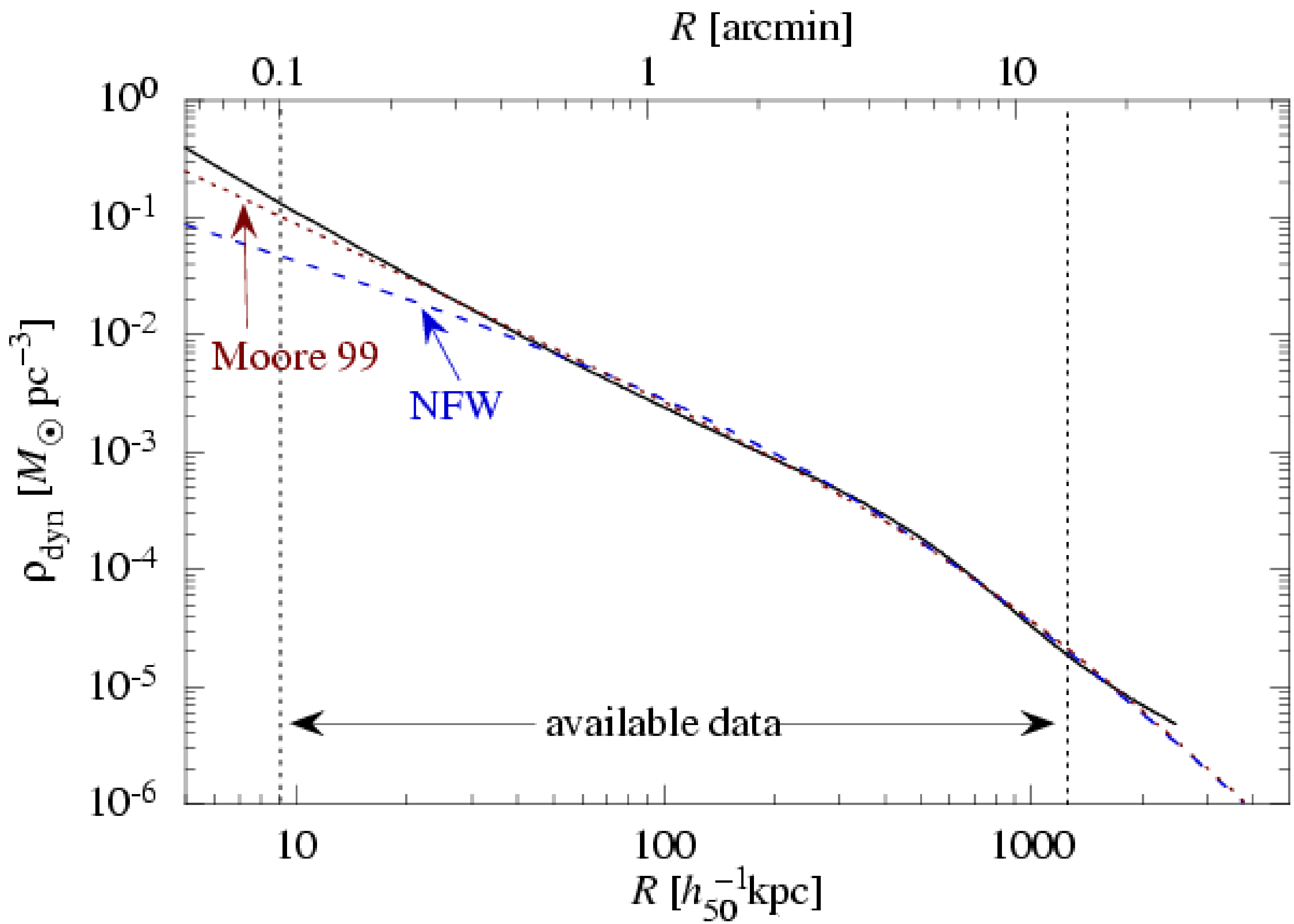

Durret et al., AA 432, 809-821 (2005)

Backgrounds -1

- Diffuse Galactic gamma-rays
  - GALPROP "conventional" model

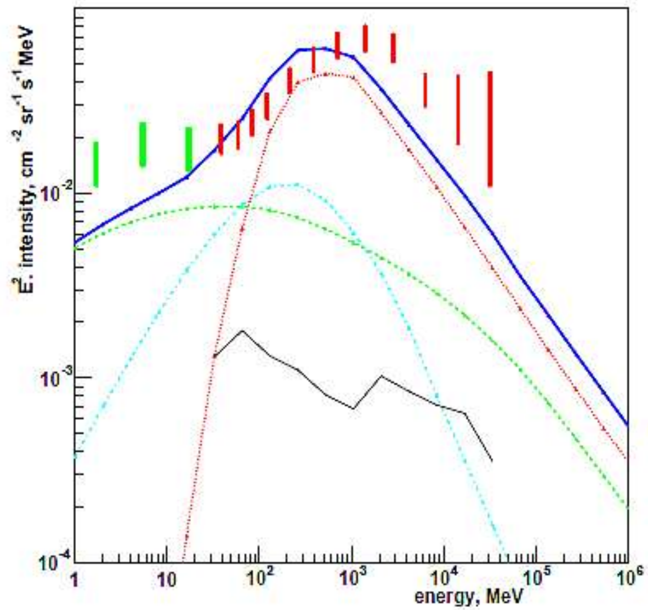

based on locally measured electron and nucleon spectra and synchrotron

pi0 decay
Inverse Compton
Bremsstrahlung
Extragalactic

Figure 3. γ-ray spectrum of the inner Galaxy ($300° < l < 30°, |b| < 5$) derived from the "conventional" model (see text for more details). Dotted: contribution from π^0 decay, dashed: contribution from inverse Compton scattering, dash-dotted: contribution from bremsstrahlung, solid: extragalactic background, bold solid: total flux. Also shown are the data points from EGRET (dark bars, red in colored versions) and COMPTEL (light bars, green in colored versions). Figure taken from [36].

Backgrounds -2

- GALPROP "optimized" model

1.8 × proton
4 × electron

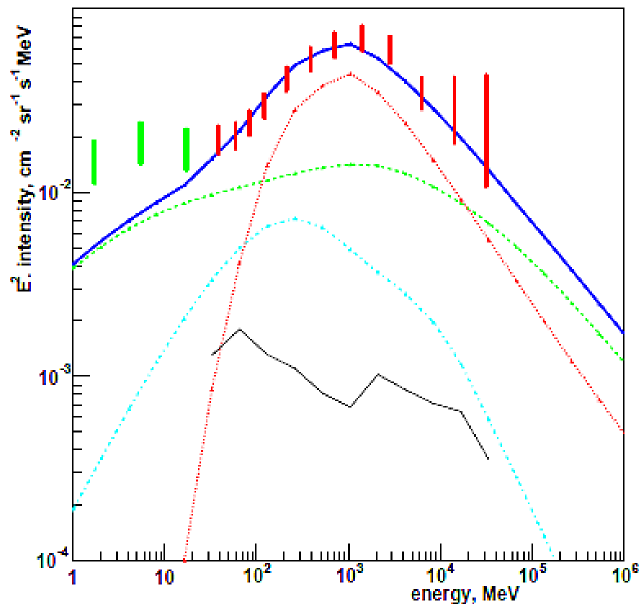

Figure 4. γ-ray spectrum of the inner Galaxy ($300° < l < 30°, |b| < 5$) derived from the "optimized" model (see text for more details). Dotted: contribution from π^0 decay, dashed: contribution from inverse Compton scattering, dash-dotted: contribution from bremsstrahlung, solid: extragalactic background, bold solid: total flux. Also shown are the data points from EGRET (dark bars, red in colored versions) and COMPTEL (light bars, green in colored versions). Figure taken from [36].

Many reasons:
•SN rate is larger in spiral arms.
•Anisotropic diffusion/convection
•Reacceleration

Backgrounds -3

- Extragalactic diffuse gamma-rays
  - Isotropic, flux comparable to IC of ISRF/CMB by CR electrons
  - Compton-scattered solar photons by CR electrons (~10%)
  - γ-ray albedo of small solar system bodies (asteroids)

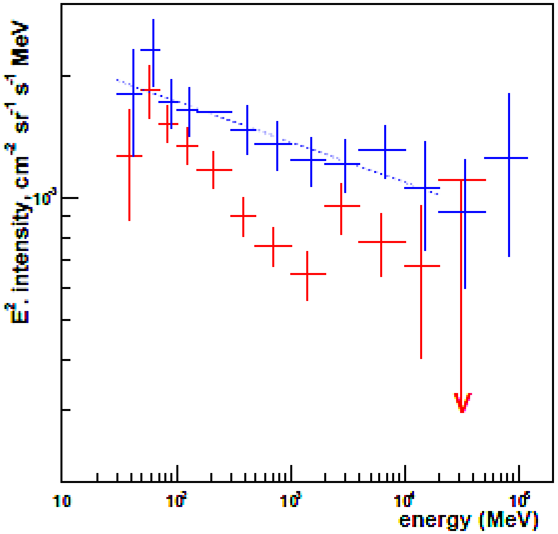

FIG. 2.— Comparison of our EGRB spectrum (solid, red) as given in Table 3 with that from Sreekumar et al. (1998) (dots, magenta). The dashed (blue) line is the Sreekumar et al. fit: $2.743 \times 10^{-3} E^{-2.1}$ cm^{-2} s^{-1} sr^{-1} MeV^{-1}.

- Sreekumar et al. (1998)
- Strong et al. (2004) with "optimized" model

Backgrounds -4

- Particle backgrounds
  - Charged particles, mainly protons, electrons and positrons, as well as a smaller number of neutrons and Earth albedo photons
  - GLAST rejection power: 10^5
- Unresolved point sources
  - <10% for EGRET, less for GLAST (weaker sources resolved)

Sensitivity for generic WIMP annihilation -1

- The Galactic center
  - TeV source
    - WIMP annihilation NOT likely
    - $2.6\times10^6 M_\odot$ black hole at the kinematic centre of our Galaxy, commonly identified with the bright compact radio source Sgr A*, or with the candidate pulsar wind nebula G359.95-0.04 recently discovered in a deep Chandra survey
  - EGRET source, 0.2° away from Sgr A*
- Task: distinguish the DM signal from a Galactic diffuse background after the astrophysical sources are disentangled and subtracted using the information provided by spectral and angular analysis and multiwavelength observations

A truncated NFW profile as defined in [24] is assumed for the WIMP distribution, and only one dominant annihilation channel (W^+W^-, $b\bar{b}$, $t\bar{t}$, $\tau^+\tau^-$) is considered at a time. Care has also been taken in order not to violate the EGRET flux constraint around the GC [77]. WIMP annihilation differential fluxes above 1 GeV and in a region of 0.5 degs radius around the GC (corresponding to the angle for 68% containment at this energy threshold) have been generated using DarkSusy v. 4.15 [78]. The expected DM from this region, incident on the LAT for 5 years of all sky scanning operation is simulated using gtobssim (see section 2.2). This flux was simulated for 10000 grid points (m_{WIMP}, $<\sigma v>$) on a 100×100 logarithmic grid. The range of chosen is $<\sigma v>\in[10^{-28},10^{-24}]$ and $m_{\mathrm{WIMP}}\in[10,3000]$ GeV for the $b\bar{b}$ and $\tau^+\tau^-$ channels, and $m_{\mathrm{WIMP}}\in[200,3000]$ for the W^+W^- and $t\bar{t}$ channels.

Sensitivity: $b\bar{b}$ channel

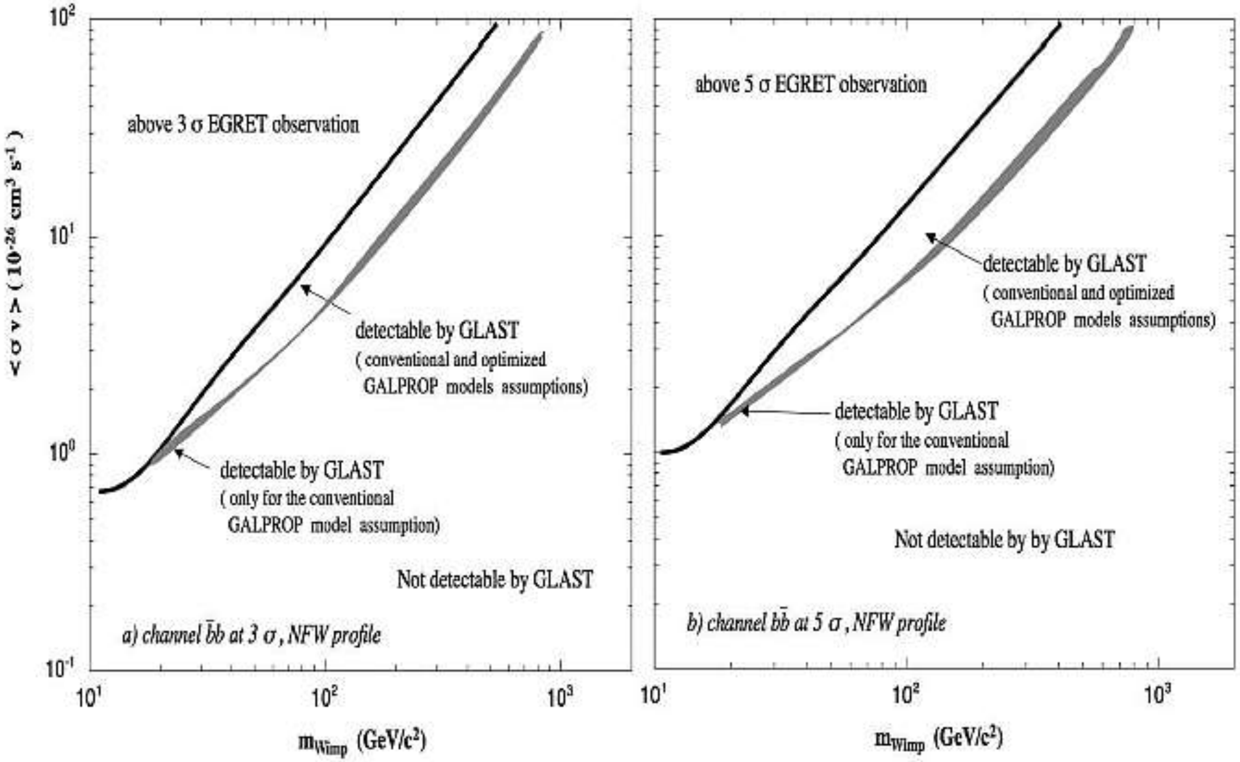

Figure 5. Cross-sections $<\sigma v>$ $(v \leftarrow 0)$ versus the WIMP mass m_{WIMP} for the $b\bar{b}$ annihilation channel. Left panel shows the result for 3σ significance, right panel shows the result for 5σ significance for **5 years of GLAST operation,** The upper part of the plots corresponds to regions which are already excluded by the EGRET data around the GC and the lower part corresponds to regions not detectable by GLAST. The "detectable by GLAST region" corresponds to models detectable by GLAST for both "conventional" and "optimized" astrophysical background. The shaded region represents models which can be detected only under the assumption of "conventional" Galactic diffuse background. See text for more details.

Sensitivity: W^+W^- channel

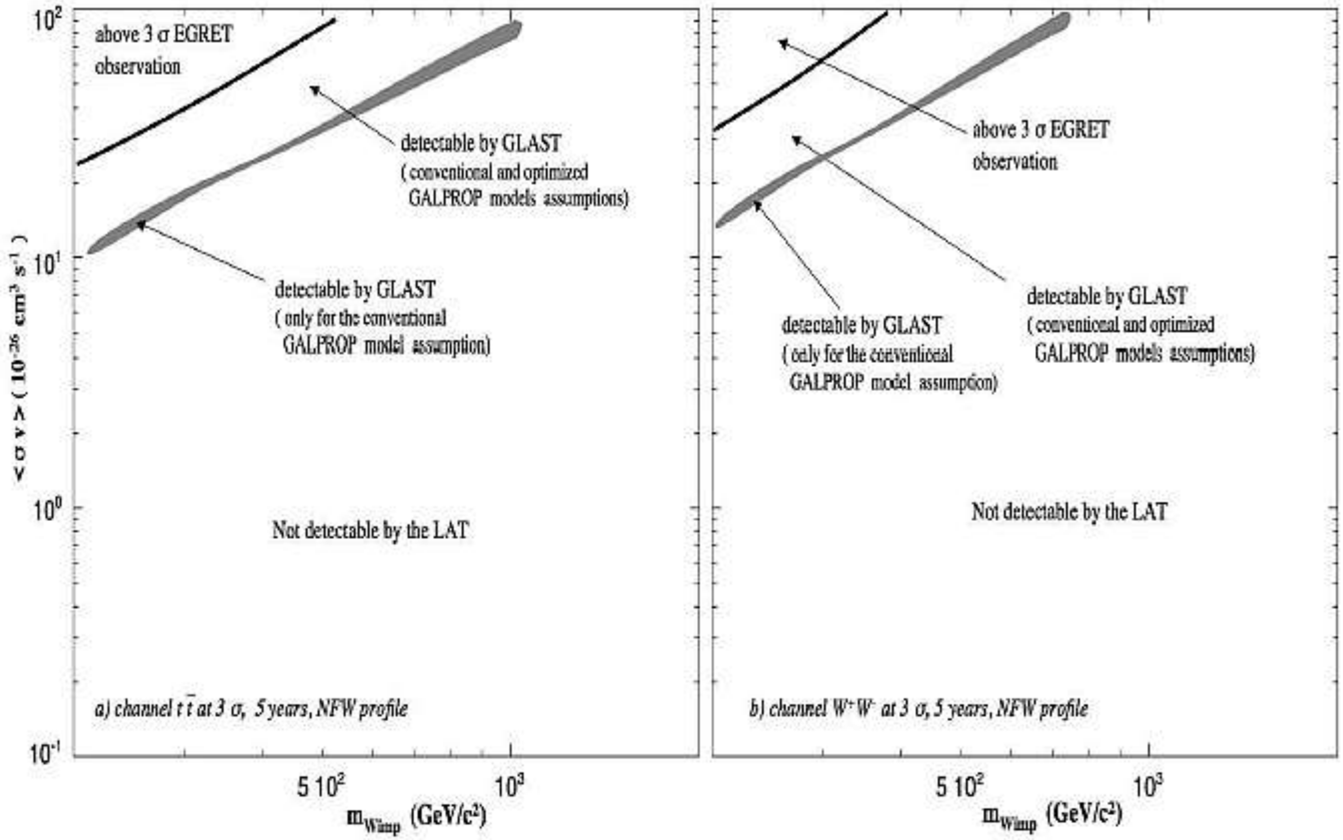

Figure 6. 3 σ sensitivity regions for the $t\bar{t}$ (left panel) and the $W^+ W^-$annihilation channel (right panel). Definitions of regions are the same as in figure 5. Note the difference in x-axis scale as compared to figure 5.

Sensitivity: $\tau^+\tau^-$ channel

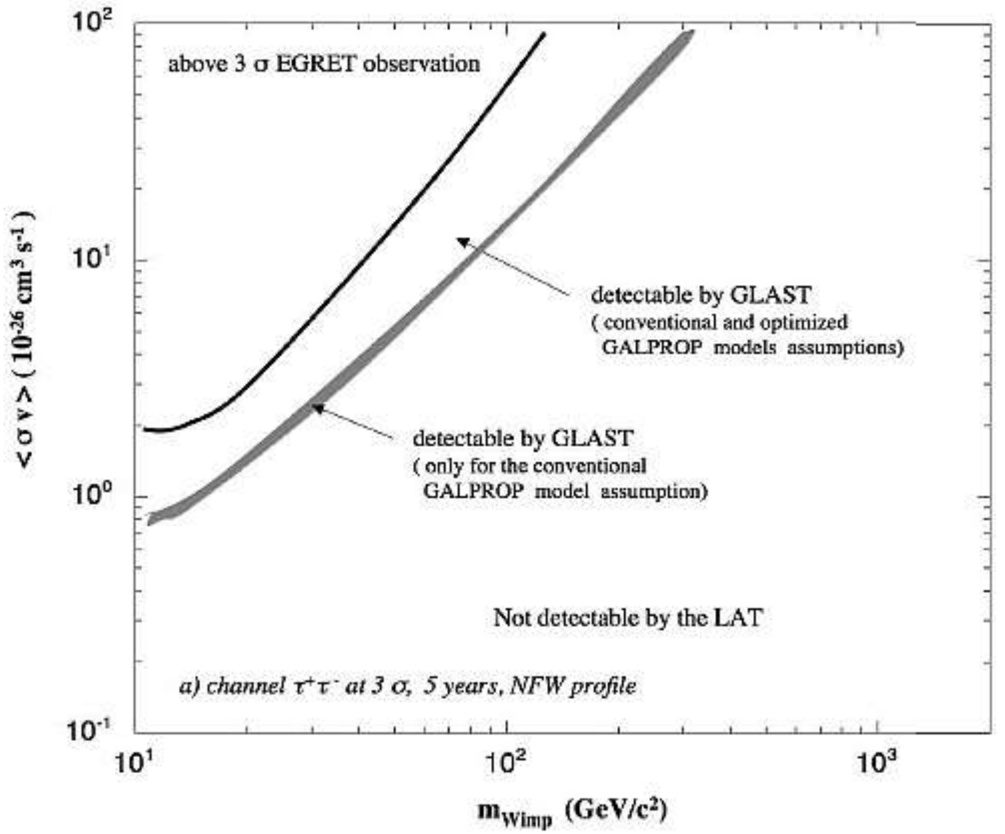

Figure 7. 3 σ sensitivity regions for the $\tau^+\ \tau^-$ annihilation channel. Definitions of regions are the same as in figure 5.

Sensitivity for generic WIMP annihilation -2

- The Galactic halo
  - Two possible exclusions:
    - (1) Region within 10° of the GC
    - (2) Region within 10° of the Galactic plane
    - Both of these choices will avoid the GC (the proposed dark matter density profiles diverge from one another).
  - "Conventional" and "Optimized" diffuse models
  - NFW profile

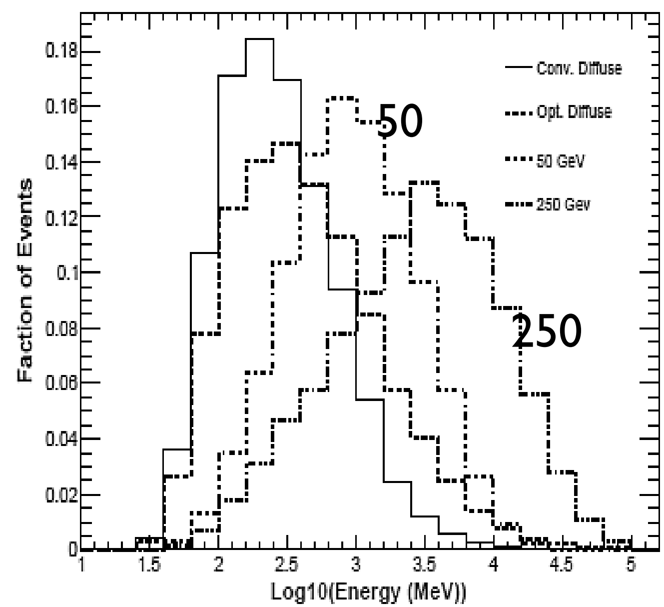

Figure 8. The energy distributions for the diffuse "conventional" and "optimized" diffuse-emission models and two DM models for WIMP masses at 50 and 250 GeV/c^2. Each distribution is individually normalized to unit area to highlight the shape differences.

→Maximum likelihood fit in energy, latitude and longitude

<σv> sensitivity

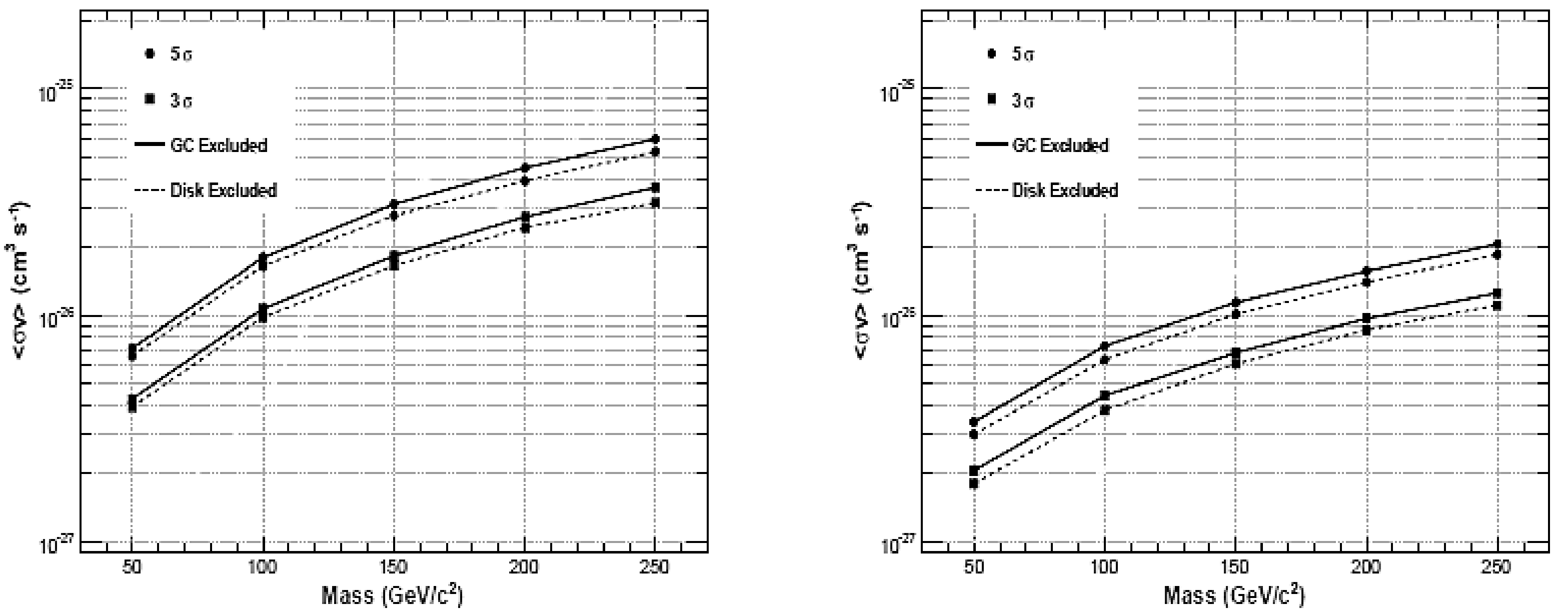

Figure 9. The $< \sigma v >$ required to obtain an observation of WIMP annihilation at either 3σ (square) and 5σ (circle) significance for **one year of GLAST data**, as a function of WIMP mass. Left panel: considering the "optimized" diffuse model as background, right panel: considering the "conventional" diffuse model. The dashed line corresponds to the 10° cut above and below the Galactic plane; the solid line corresponds to a 10° radial cut around the Galactic center.

Example of pseudoexperiments

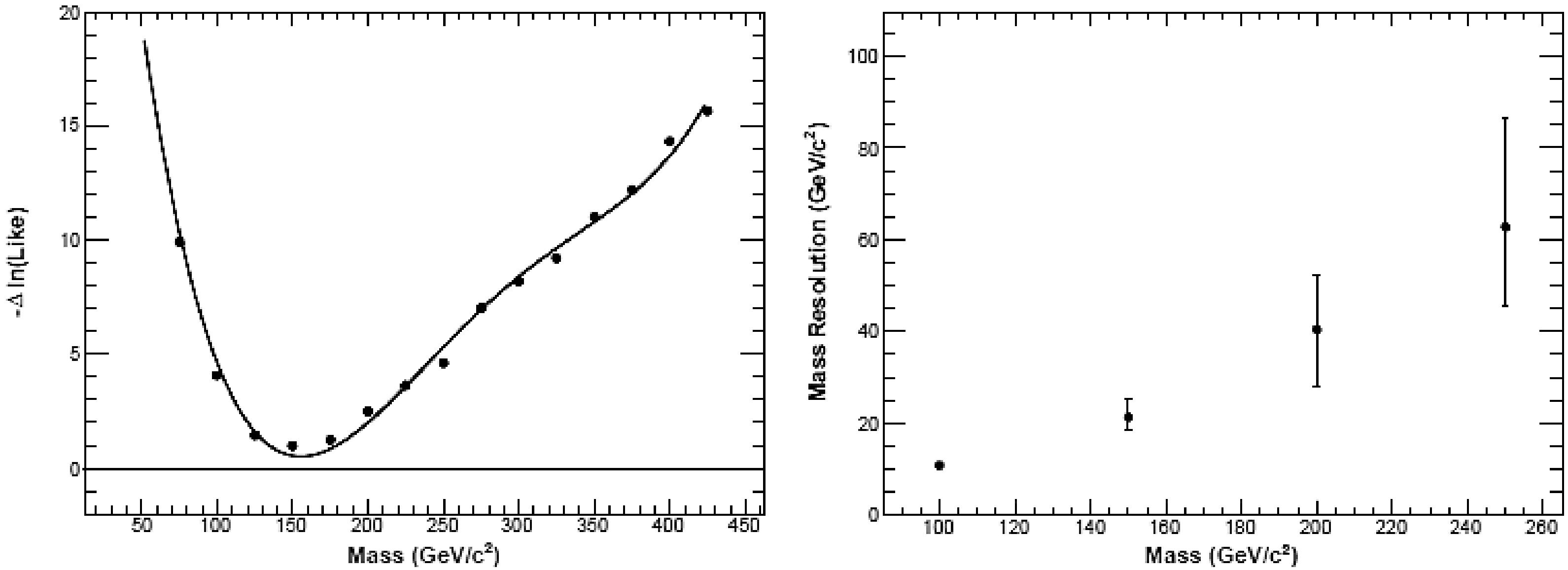

Figure 10. The left plot shows the fitted $-\Delta$ log-likelihood versus mass for a single pseudo-experiment assuming the true mass of the WIMP to be 150 GeV/c^2. The resulting fitted mass for this pseudo-experiment is 155 ± 23 GeV$/c^2$. The right plot shows the mean fitted error returned by the fit, versus the true WIMP mass. The error bars show the 68% containment interval for the pseudoexperiments, which demonstrates the range of possible outcomes from a single experiment. The parameters describing the pseudoexperiments are given in the text.

Sensitivity for generic WIMP annihilation -3

- Galactic satellites
  - Galactic sub-halos
    - Hierarchical structure formation in CDM models → Large number of sub-halos, $(10^{-4} – 10^{-12})M_{\odot}$, nearly isotropic
  - Dwarf galaxies
    - Largest clumps predicted by the CDM scenario
- Point sources
    - Intermediate size black holes, i.e. wandering black holes with masses $10^2 < M/M_{\odot} < 10^6$, which would adiabatically grow "mini-spikes" of DM.

Number of observable DM satellites

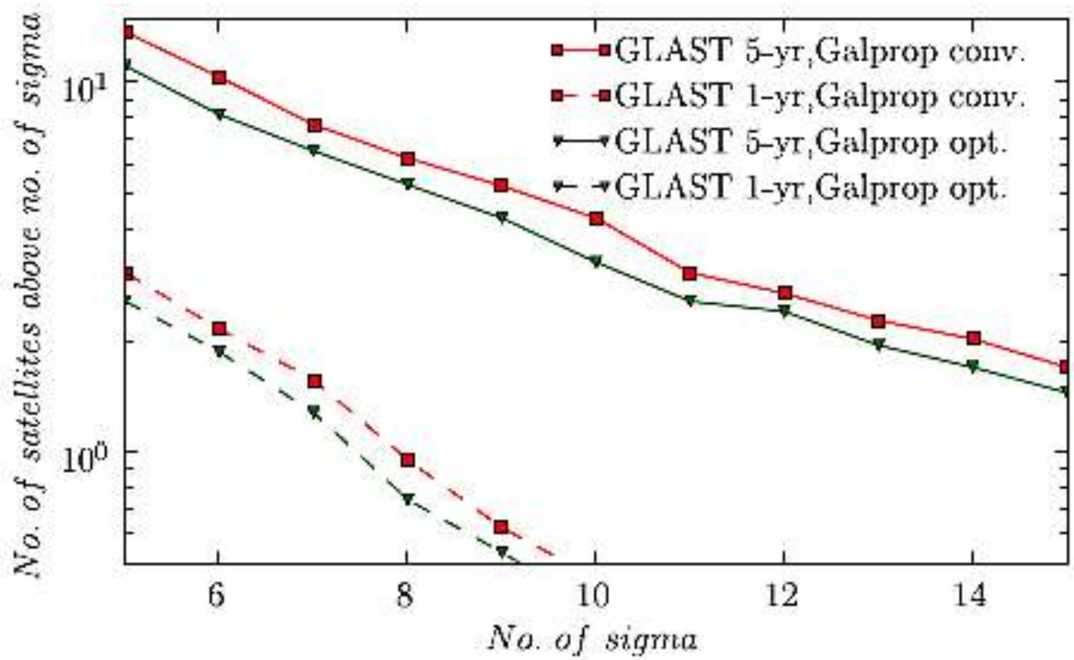

Figure 11. Estimated number of observable DM satellites for the LAT in the Milky Way for **1 and 5 year of GLAST operation**. The background consists of the isotropic extragalactic diffuse [54] and GALPROP "conventional" / "optimized" Galactic diffuse model. The significance is estimated as $N_S/\sqrt{N_S+N_B}$ within the satellite tidal radius (or the PSF 68% containment radius if larger) at $E_\gamma > 1$ GeV.

Spectra for WIMP satellites

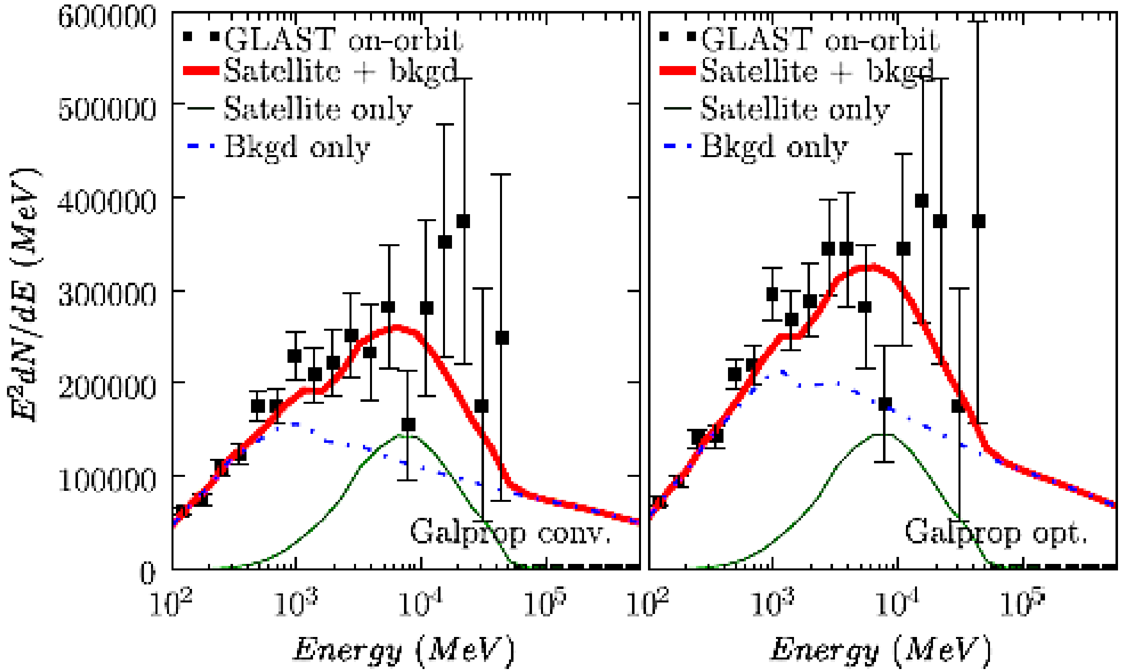

Figure 13. Counts spectra for the same generic WIMP satellite within its tidal radius. The squares with 1 sigma error bars show the spectrum of simulated **1 year GLAST data**. The thick lines show the background plus the satellite signal. The thin lines show the satellite predictions only. The dash-dot lines show the background predictions only.

Distinguishing WIMP satellites from background

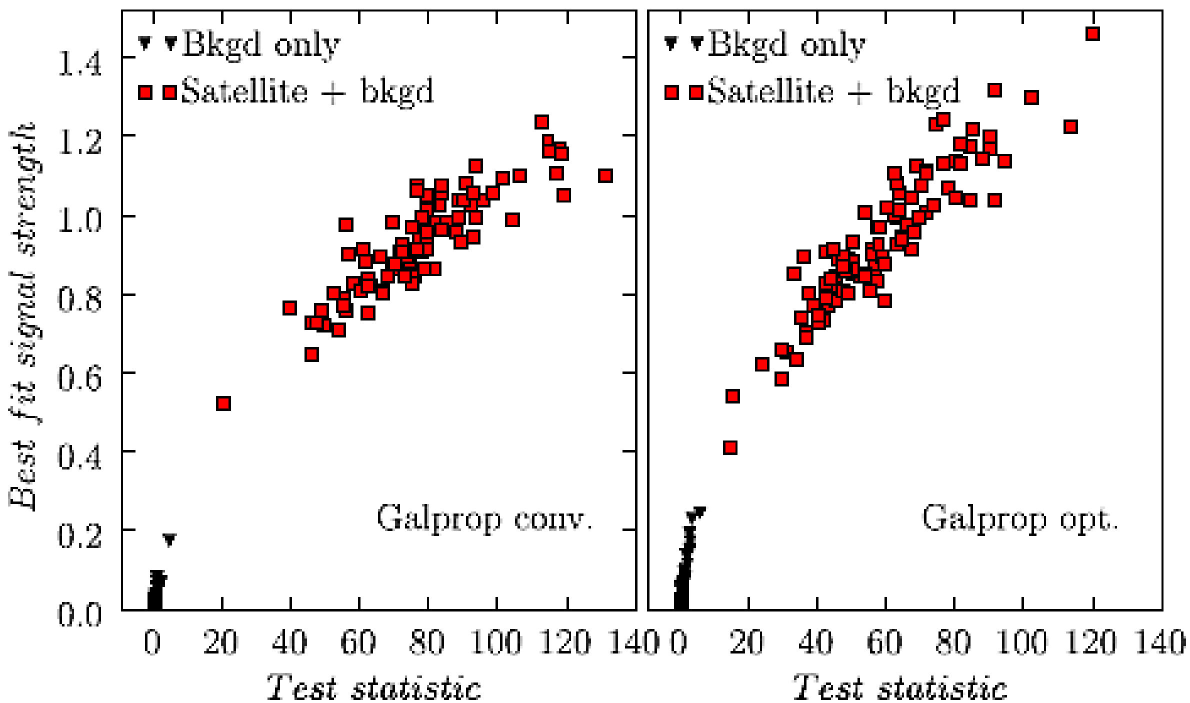

Figure 14. Null hypothesis test to distinguish the same generic WIMP satellite from a background fluctuation. The test statistics for background only and for background plus satellite signal could be separable.

Sensitivity to Sagittarius Dwarf

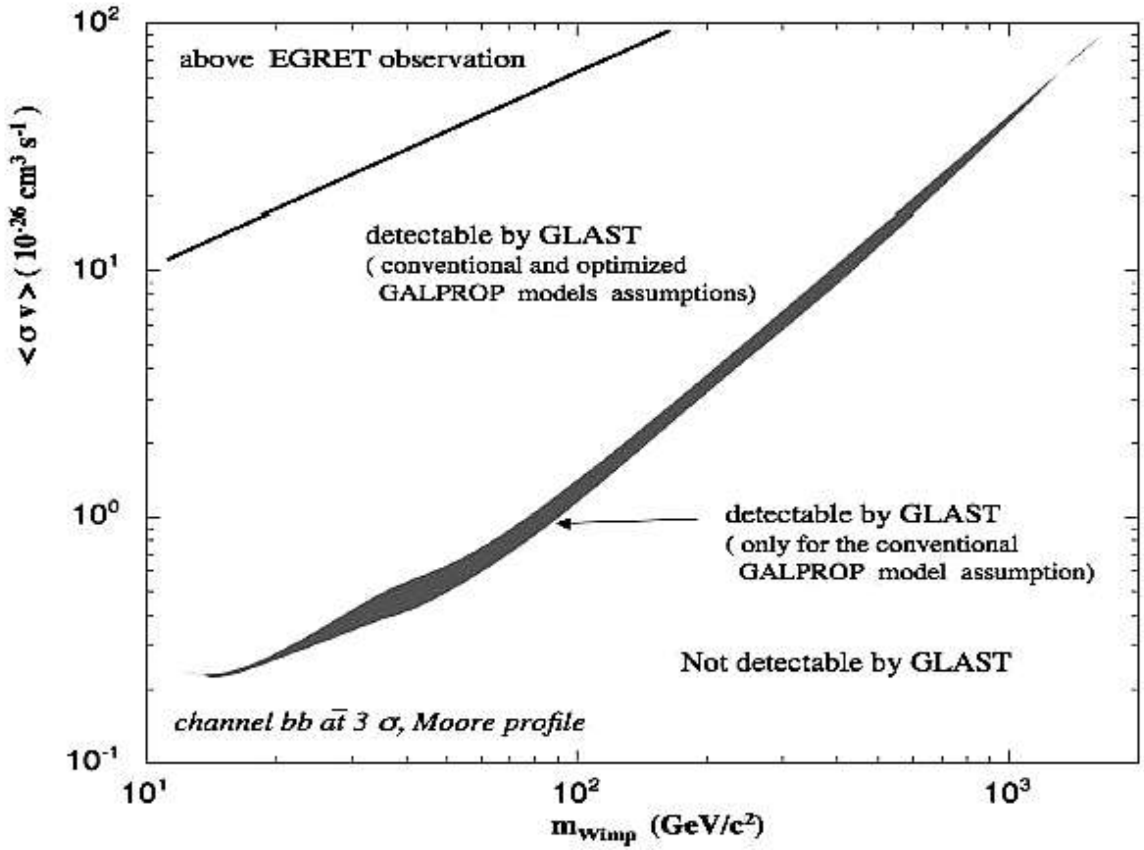

Figure 15. Sensitivity to a Sagittarius Dwarf DM signal for **5 years of GLAST operation** assuming Moore profile as described in [95]. The region labeled "above EGRET observation" is calculated with respect to the upper limit map provided in [96].

LAT error ellipses for DM satellites

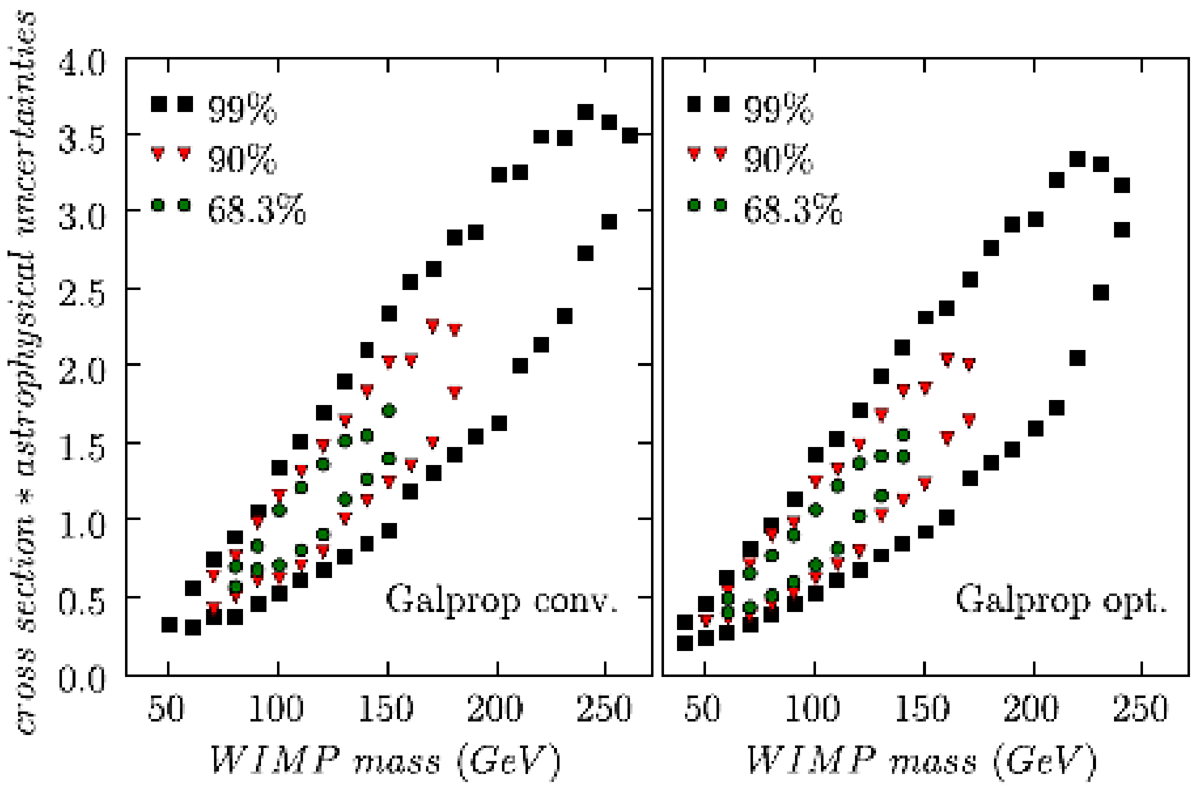

Figure 12. LAT error ellipses for a simulated "5 sigma" DM satellite with the generic WIMP model. The vertical axis is given by Equation (4).

Flux needed for separating a DM point source

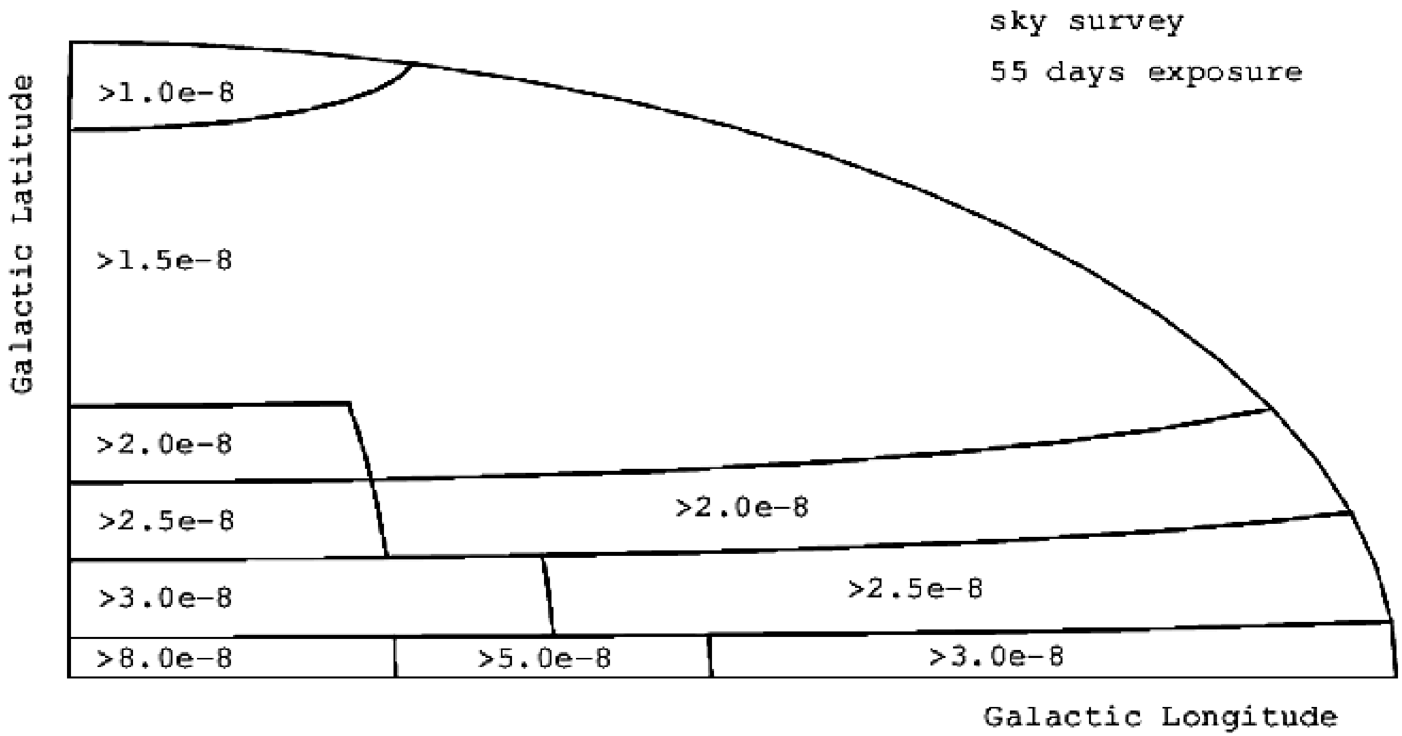

Figure 16. Flux needed for separating a point sources of DM annihilation from the background, i.e. full-sky map in Galactic coordinates of the minimum flux above 100 MeV, in units of [ph $cm^{-2}s^{-1}$], that is required for a 5σ detection of an annihilation spectrum, assuming a DM particle with mass $m_{WIMP} = 150$ GeV annihilating into $b\bar{b}$ (note, however, that the map does not depend very sensitively on DM properties). The map is relative to **a 2 month operation period**; for longer operation times, fluxes scale approximately as $t_{obs}^{-1/2}$.

Spectral fits of DM point sources

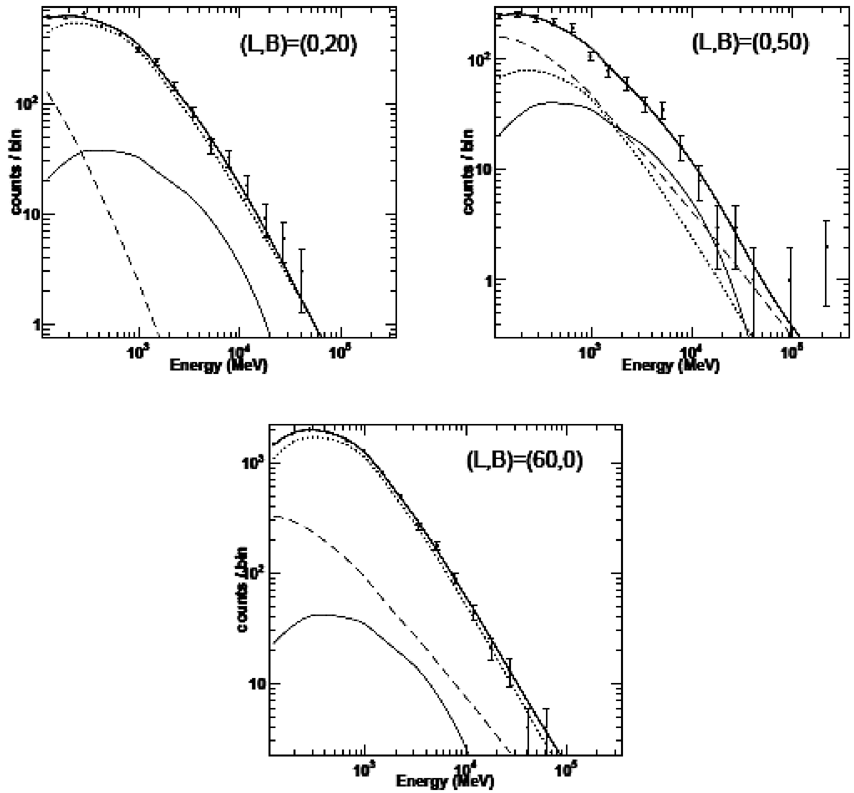

Figure 17. Examples of spectral fits of simulated DM point sources of intensity $\phi = 8 \cdot 10^{-8}$ ph cm^{-2}s^{-1} above 100 MeV, $m_{WIMP} = 150$ GeV $b\bar{b}$ annihilation channel. Upper left for (l,b) = (0,20); upper right for (l,b)= (0,50) and on the bottom (l,b)=(60,0). Thin solid lines: DM signal, dashed: Galactic diffuse contribution, dotted: extragalactic contribution (from [54]), points with error bars are photon counts from the simulated observation.

Line signal sensitivity

- Line signal from $\chi\chi\rightarrow\gamma\gamma$ at half the DM mass
  - "smoking gun" for WIMP DM
  - Branching ratio: ~10^{-3} or less

LAT energy dispersion

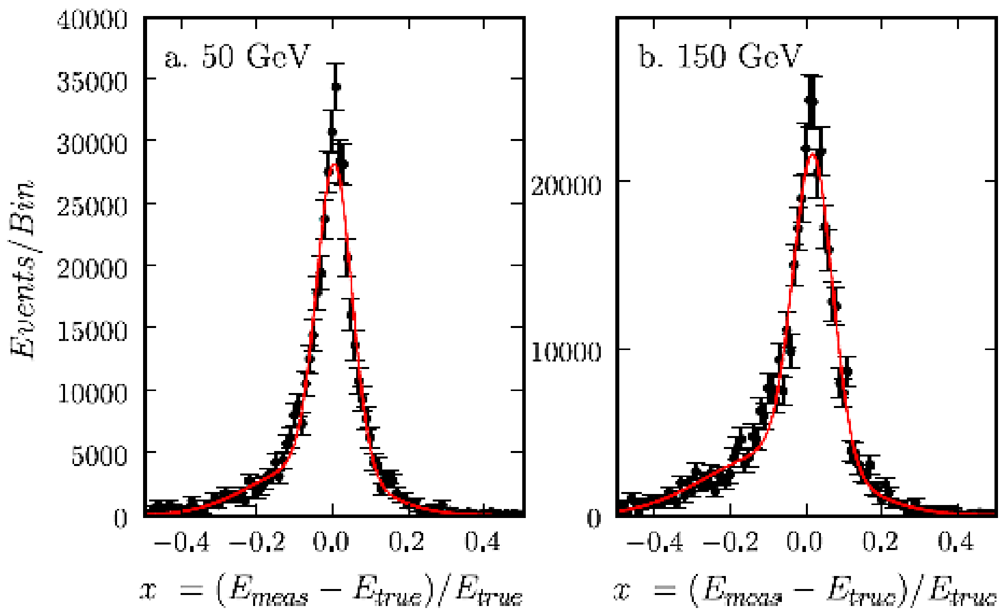

Figure 18. Double Gaussian fits to the simulated LAT energy dispersion for γ-ray energies of a) 50 and b) 150 GeV.

Spectral fit -1

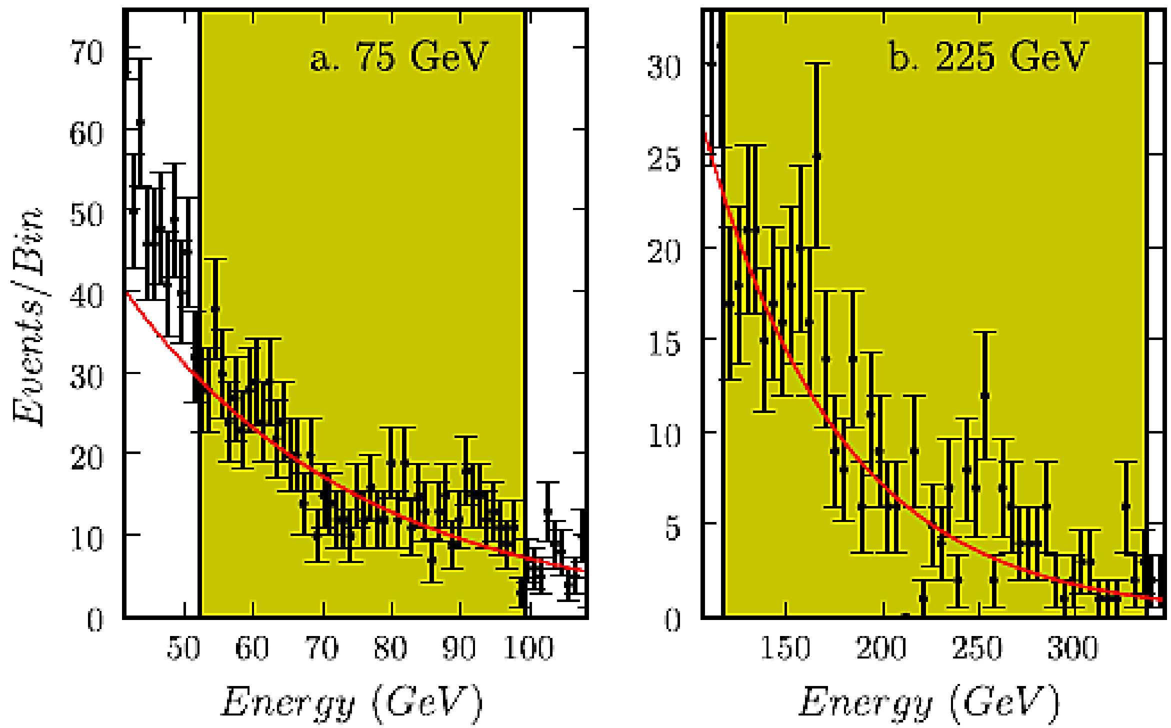

Figure 19. "Conventional" Galactic plus extragalactic background fit to a powerlaw over the range $[E_0 - 6\sigma_E, E_0 + 6\sigma_E]$, for a) $E_0 = 75$ GeV and b) $E_0 = 225$ GeV. The fit range is shown as a shaded area.

Spectral fit -2

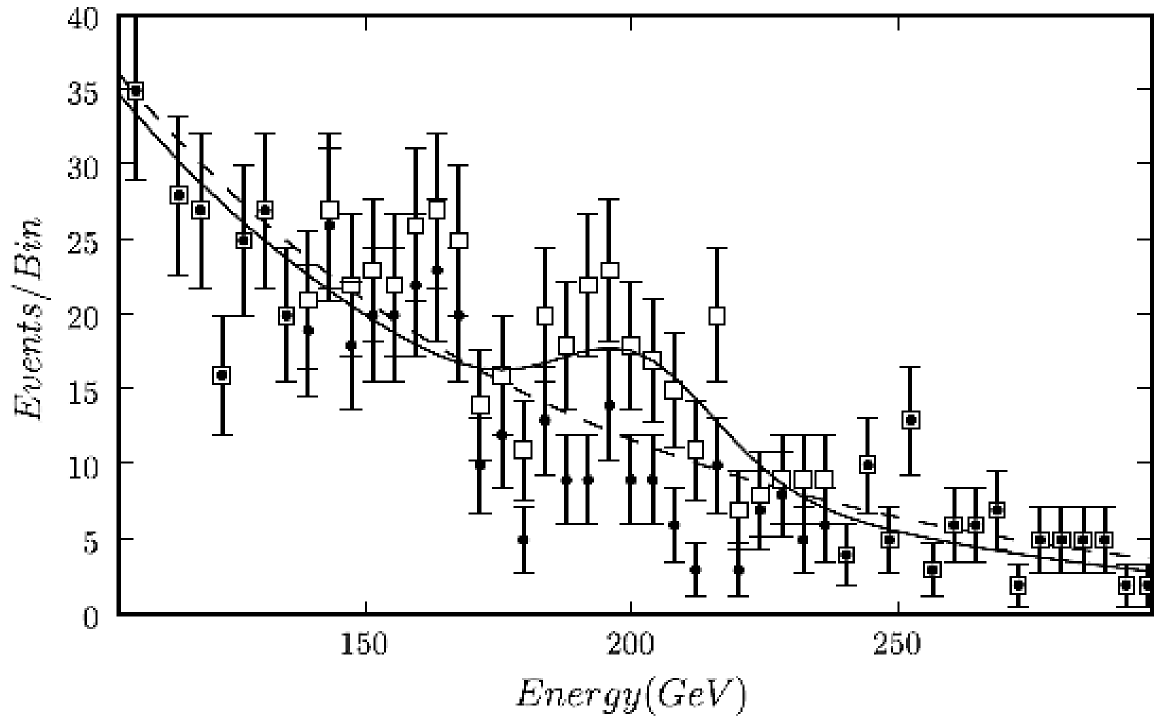

Figure 20. "Optimized" diffuse background and a 5σ signal at 200 GeV. The black dots and open squares correspond to the diffuse background and the diffuse background plus MC signal, respectively. Full and dotted lines correspond to the signal plus background fit to $\phi 2$ and $\phi 1+\phi 2$, respectively. $< \Delta\chi^2 >= 25.0$ for this run.

Sensitivity contours

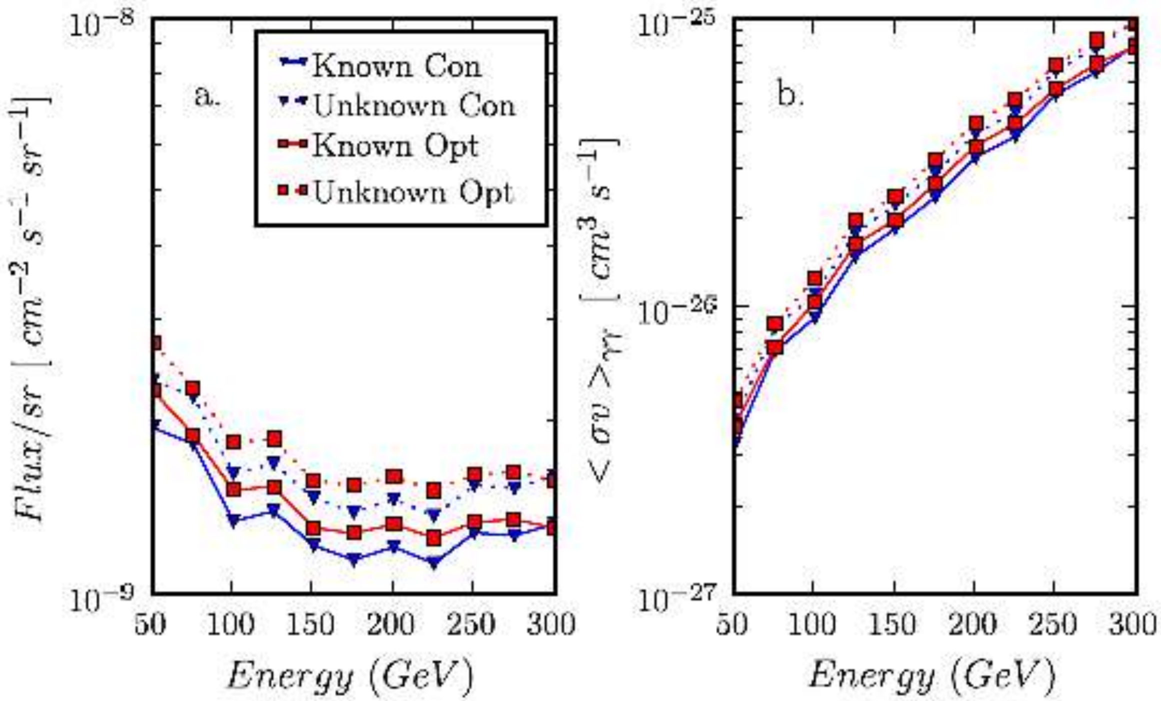

Figure 21. 5σ sensitivity contours **(5 years of GLAST operation)** in a) flux and b) velocity-averaged effective cross-section. Triangles and squares correspond to the "conventional" and "optimized" Galactic background model, respectively. Full and dotted lines correspond to the case of known and unknown WIMP energy, respectively.

Upper limit contours

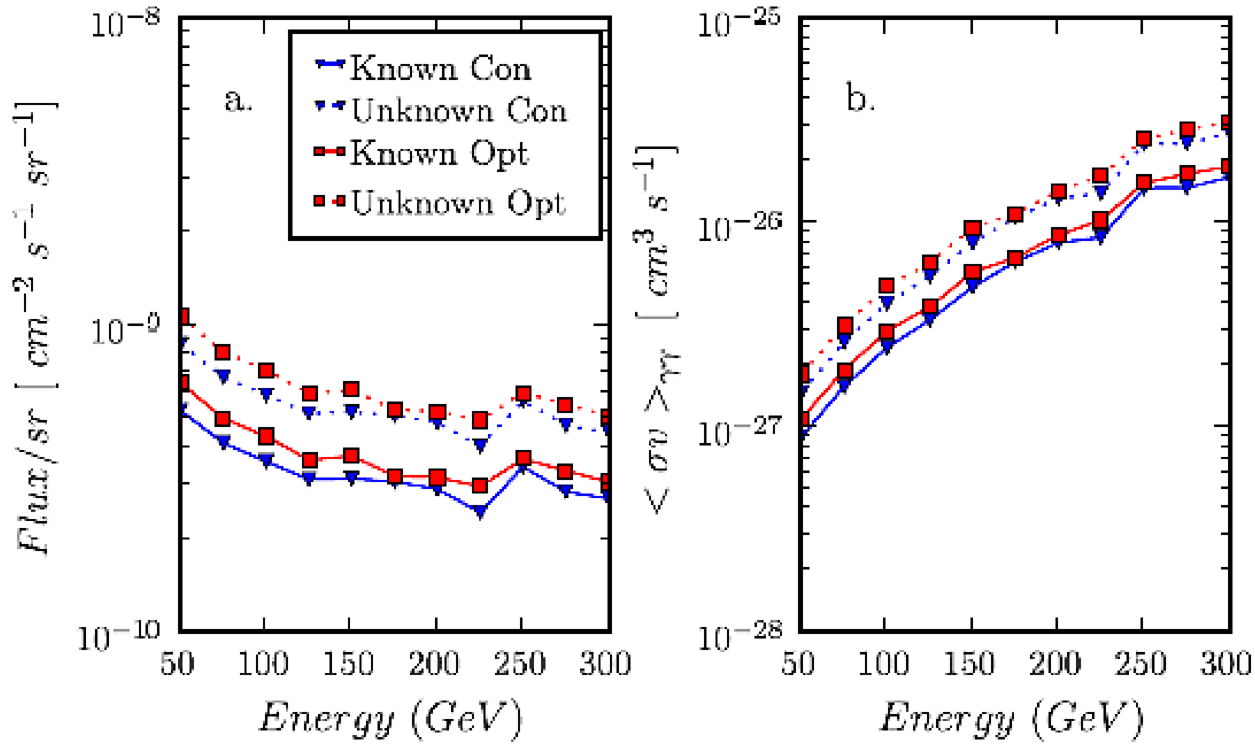

Figure 22. 95% confidence level upper limit contours **(5 years of GLAST operation)** in a) flux and b) velocity-averaged effective cross-section, as a function of the WIMP energy. The legend is identical to figure 21.

Cosmological WIMP annihilation: Extragalactic background spectrum

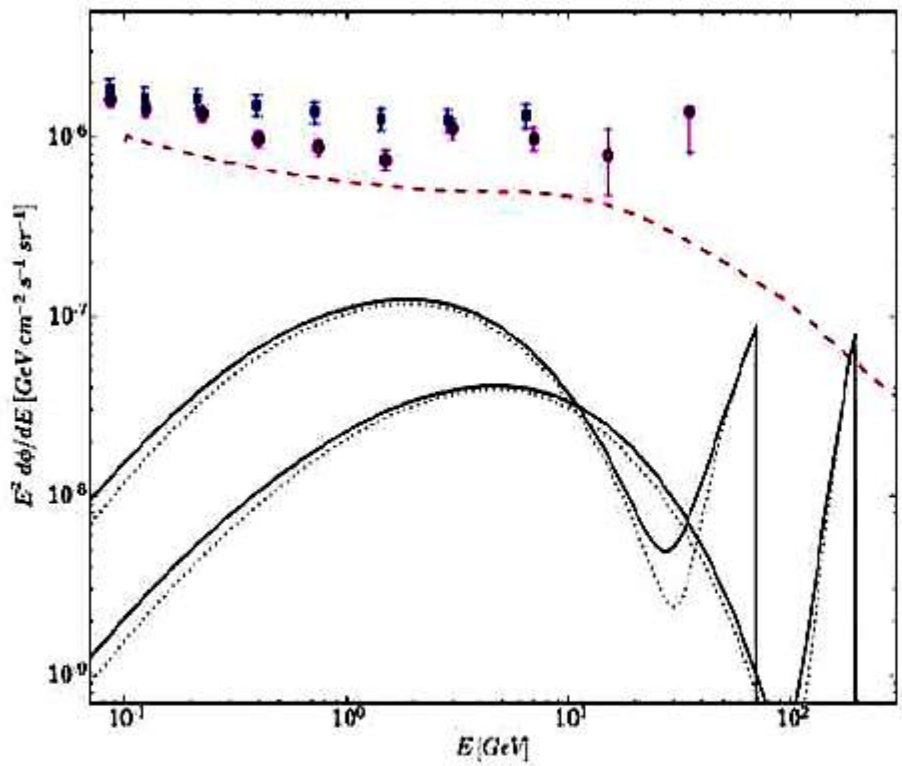

Figure 23. Spectral shapes of the EGRET measurements of the EGRB,[54] used as our conservative background (dots) and [55] (squares), the unresolved blazar model (dashed) [101], and two examples of cosmological WIMPs, Equation (10) (including the effect of substructures, see text), with masses of 70 and 200 GeV. The dotted WIMP spectra are calculated with the absorption from [103].

Exclusion curves

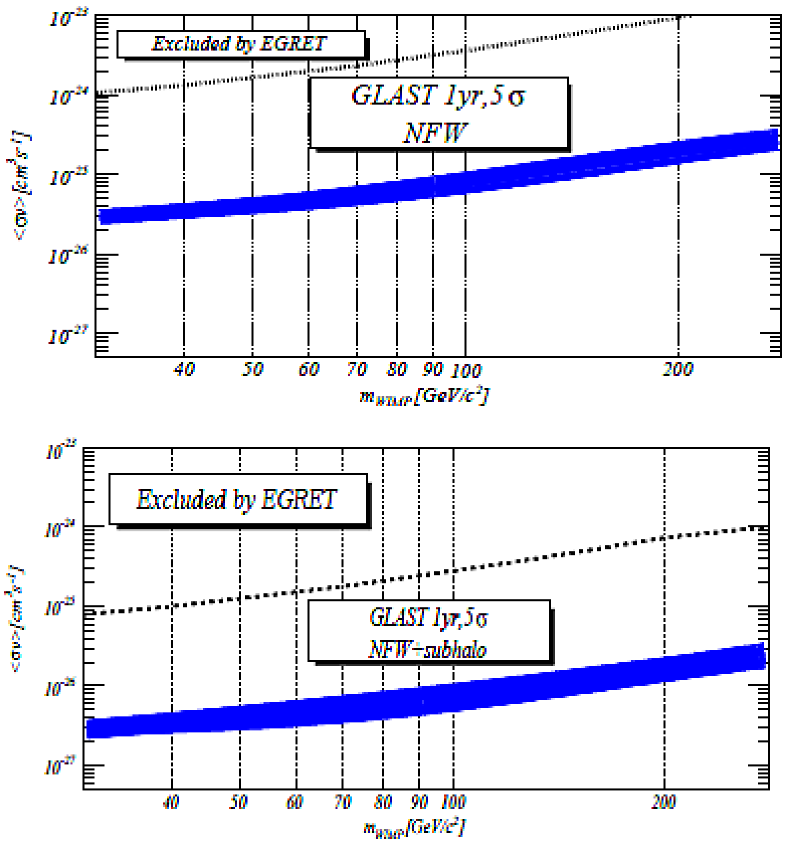

Figure 24. 5σ exclusion curves for one year of GLAST simulated data. The lower edge of the shaded band corresponds to a background as predicted by the Blazar model presented by [101], and the upper bound corresponds to the conservative case, where the background flux is given by the analysis of EGRET data [54]. NFW denotes computation of the WIMP signal using a NFW profile [27] and NFW+subhalo includes the effect of having 5 % of the host halo mass in substructures with four times higher concentration parameter than the parent halo. Note that a Moore profile would lead to an improvement in sensitivity by about a factor of ten.

GLAST sensitivity to specific particle physics models -1

- mSUGRA (constrained version of MSSM: minimal supersymmetric standard model)

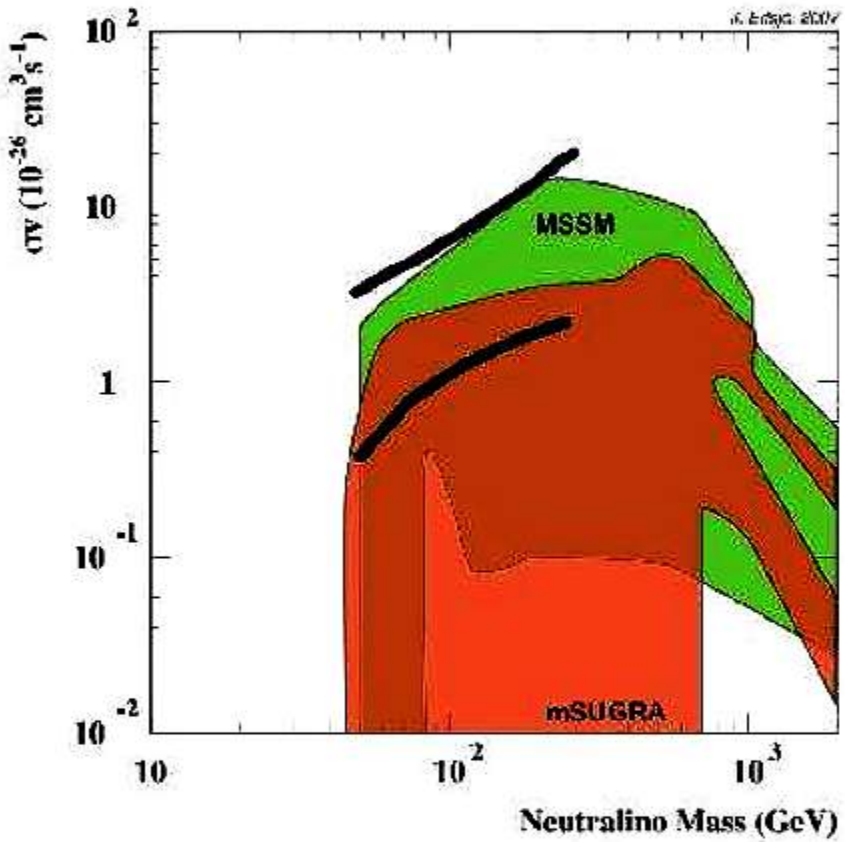

Figure 25. MSSM and mSUGRA models in the $< \sigma v >, m_{WIMP}$ plane. The models included in these regions are consistent with accelerator constrains and WMAP data. The lines represent the 5 σ sensitivity from the GC (upper) and the 5 σ sensitivity from a Galactic halo analysis (lower) corresponding to the best and worst sensitivities estimated in this paper for a NFW profile.

GLAST sensitivity to specific particle physics models -2

- UED (Universal Extra Dimension)
  - Lightest Kaluza-Klein Particles (LKP)

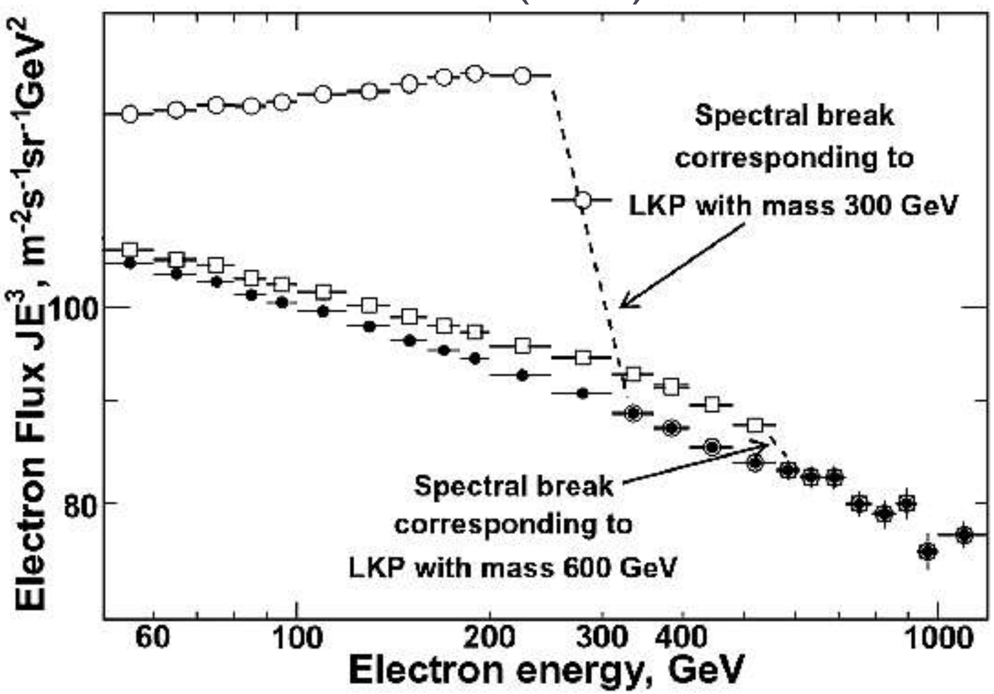

Figure 29. Simulated detection of LKPs with masses of 300 GeV and 600 GeV in the LAT electron spectrum to be collected in **5 years of operation**. Filled circles — "conventional" electron flux; open circles — the same but with added signal from 300 GeV LKP, and open squares — the same with added signal from 600 GeV LKP. For this signal, only the nearest clump at a distance of 100 pc is considered. The breaks are also shown by dashed lines to guide the eye.

Conclusion

- Using the current state-of-the-art Monte Carlo and event reconstruction software developed within the LAT collaboration, we present preliminary sensitivity calculations for several astrophysical searches of DM annihilation.
- LAT has good potential to discover DM annihilation for a significant fraction of interesting parameter space, i.e. for values of annihilation cross-section of between $<\sigma v>\simeq 10^{-26}$ $cm^3 s^{-1}$ and $<\sigma v>\simeq 10^{-24}$ $cm^3 s^{-1}$ depending on WIMP masses in the range between 40 and 500 GeV.
- For less conservative assumptions on the Dark Matter density (for example additional substructure or a Moore profile) the sensitivity improves by one to two order of magnitudes.